

# Substrate twinning activates the signal recognition particle and its receptor

Pascal F. Egea<sup>1</sup>, Shu-ou Shan<sup>1,2</sup>, Johanna Napetschnig<sup>1</sup>, David F. Savage<sup>1</sup>, Peter Walter<sup>1,2</sup> & Robert M. Stroud<sup>1</sup>

<sup>1</sup>Department of Biochemistry and Biophysics, University of California at San Francisco, California 94143-2240, USA

<sup>2</sup>Howard Hughes Medical Institute, San Francisco, California 94143, USA

**Signal sequences target proteins for secretion from cells or for integration into cell membranes. As nascent proteins emerge from the ribosome, signal sequences are recognized by the signal recognition particle (SRP), which subsequently associates with its receptor (SR). In this complex, the SRP and SR stimulate each other's GTPase activity, and GTP hydrolysis ensures unidirectional targeting of cargo through a translocation pore in the membrane. To define the mechanism of reciprocal activation, we determined the 1.9 Å structure of the complex formed between these two GTPases. The two partners form a quasi-two-fold symmetrical heterodimer. Biochemical analysis supports the importance of the extensive interaction surface. Complex formation aligns the two GTP molecules in a symmetrical, composite active site, and the 3'OH groups are essential for association, reciprocal activation and catalysis. This unique circle of twinned interactions is severed twice on hydrolysis, leading to complex dissociation after cargo delivery.**

The SRP and its receptor (SR) target nascent proteins destined for secretion or membrane integration to the endoplasmic reticulum (ER) membrane in eukaryotes or to the plasma membrane in prokaryotes<sup>1,2</sup>. The principal components of SRP and SR are conserved across all kingdoms. In prokaryotes the SRP is a ribonucleoproteinaceous complex consisting of a single 48 kDa GTPase, Ffh (the orthologue of the eukaryotic SRP54), and a 110-nucleotide 4.5S RNA (the orthologue of the eukaryotic 7SL RNA), whereas SR consists of a single GTPase called FtsY.

SRP54 associates with ribosomes near the peptide exit site<sup>3</sup>, and binds to signal sequences of membrane and secretory proteins as they emerge from the ribosome during translation<sup>4</sup>. SRP, with its ribosome and nascent polypeptide as cargo, then binds to SR (or FtsY)<sup>5,6</sup>, which in turn is dynamically associated with the Sec61 (or SecYEG) translocon in the target membrane. Thus, SRP and SR act as molecular matchmakers to deliver the nascent polypeptide to the translocon. At the membrane, the ribosome and nascent polypeptide are released from SRP<sup>5,7,8</sup> and bound instead by the translocon<sup>9–11</sup>. SRP and SR reciprocally stimulate each other's GTPase activity, leading to dissociation of the complex<sup>12–14</sup>.

Ffh comprises three domains, termed N, G and M<sup>15</sup>. The M domain contains the signal-sequence-binding site and provides a primary contact with 4.5S RNA, and is connected to the N and G domains by means of a flexible linker. The amino-terminal N domain and the GTPase G domain are structurally and functionally coupled in an arrangement that is universally conserved between all SRP GTPases<sup>16</sup>. The N domain is a four-helix bundle<sup>16,17</sup> that changes its angle relative to the G domain depending on the nucleotide-bound state of the G domain<sup>18</sup>. The G domain is a Ras-like GTPase<sup>17,19</sup> with an additional  $\beta$ - $\alpha$ - $\beta$ - $\alpha$  insertion box domain (IBD) that is unique to the SRP subfamily of GTPases<sup>17,20</sup> (Fig. 1a). The N and G domains of both Ffh and FtsY are sufficient for stable complex formation in the presence of the non-hydrolysable GTP analogues GMPPCP or GMPPNP. The structure of the complex reported here with GMPPCP elucidates a new mechanism by which complex formation activates both GTPases, and explains how subsequent GTP hydrolysis would break the interaction and cause dissociation of Ffh from FtsY. Each GTPase provides its own catalytic machinery *in cis* and is stimulated *in trans* by hydrogen bonds between the twinned GTPs.

## The Ffh–FtsY heterodimer association

The X-ray structure of the catalytic core formed by the *Thermus aquaticus* SRP receptor (FtsY) and the N and G domains of the SRP protein (Ffh) in the presence of the non-hydrolysable GTP analogue GMPPCP was determined to 1.9 Å resolution (Table 1). The two GTPases form a quasi-two-fold symmetrical heterodimer through a continuous interface that surrounds the two bound GTPs and involves the G and N domains of both proteins (Fig. 1b, c). The primary interaction is between the G domains of FtsY and Ffh, and accounts for 2,500 Å<sup>2</sup> of the total 3,200 Å<sup>2</sup> buried surface area, whereas the N domains interact mostly with each other, and their

Table 1 Crystallographic data collection and refinement statistics

Data set	ALS 8.3.1 native
Wavelength (Å)	1.00
Resolution (last shell) (Å)	50–1.9 (1.97–1.9)
Total reflections	305,159
Unique reflections	47,344
Redundancy	6.3
Completeness (last shell) (%)	99.3 (97.9)
$R_{\text{sym}}$ (last shell) (%)	7.7 (76.7)
$I/\sigma$ (last shell)	16.9 (3.1)
Refinement statistics	FtsY–Ffh–GMPPCP complex
Reflections in working set (92.5% at $2\sigma$ )	41,806
Reflections in test set (7.5% at $2\sigma$ )	3,436
$R_{\text{cryst}}$ (%)	20.6%
$R_{\text{free}}$ (%)	23.9%
r.m.s.d. bonds (Å)	0.005
r.m.s.d. angles (°)	1.4
FtsY and Ffh	
Non-hydrogen protein atoms	2,091 and 2,183
Non-hydrogen ligand atoms	32 and 32
Ions (magnesium)	1 and 1
Solvent molecules	387
Average B-factors (Å <sup>2</sup> )	
B-Wilson from data	13
Overall protein	22 and 22
Overall G domains	16 and 18
Overall N domains	32 and 35
Ligand atoms (including Mg <sup>2+</sup> ion)	14 and 14
Solvent molecules	31

r.m.s.d. is the root mean square deviation from ideal geometry.  $R_{\text{sym}} = \sum_i \sum_j |I_{hkl,i} - I_{hkl,j}| / \sum_i \sum_j I_{hkl,i}$ , where  $I_{hkl,i}$  is the average intensity of the multiple  $hkl,i$  observations for symmetry related reflections.  $R_{\text{cryst}} = \sum_i |F_o - F_c| / \sum_i F_o$ .  $F_o$  and  $F_c$  are observed and calculated structure factors,  $R_{\text{free}}$  is calculated from a set of randomly chosen 7.5% reflections ( $2\sigma$ ), and  $R_{\text{cryst}}$  is calculated over the remaining 92.5% of reflections ( $2\sigma$ ).

interaction surface accounts for 700 Å<sup>2</sup> (Fig. 2), suggesting that complex formation is driven primarily by the pairing of G domains.

The interface is stabilized by extensive pairing interactions between Ffh and FtsY (Fig. 2a): 39 residues of FtsY and 34 residues of Ffh form 21 hydrogen bonds (10 direct and 11 water-mediated) and 139 van der Waals contacts. Three major areas of the interface are contributed to by residues interacting with each other across the quasi-two-fold axis (Fig. 2b, orange arrows, and Fig. 2c): (1) residues from motif II (Fig. 1) form extensive van der Waals contacts; (2) the N-terminal ends of the α3 helices come into close contact at the position of two conserved glycine residues; and (3) the conserved 'ALLEADV' motifs in the N domains that pack tightly against the base of the G domain are linked by means of an extensive network of interactions with α3 and α4 helices of the binding partner. There are no cavities in the interface with the single exception of the region localized between the two CH<sub>2</sub> groups of the GMPPCP molecules (see below). The sequestration of bound GTPs from solvent rationalizes the observation that there is no dissociation of GTP from the complex without GTP hydrolysis and concomitant dissociation of the complex<sup>21,22</sup>.

An independent biochemical analysis of the Ffh–FtsY interaction agrees with the structure of the complex. This analysis was performed with *Escherichia coli* FtsY, which is highly homologous to *T. aquaticus* FtsY and on which most functional studies have been performed. Mutagenesis was carried out on conserved surface residues. Each of 40 mutant proteins was purified and assayed *in vitro*. A large proportion of the mutant FtsY proteins severely compromise the reciprocally stimulated GTPase reaction of FtsY with Ffh. The second-order rate constant ( $k_{\text{tot}}$ ) for the reaction GTP·Ffh + FtsY·GTP → products, which includes both complex

formation and activation of GTP hydrolysis, is reduced 5–10<sup>3</sup>-fold in 25 out of the 40 mutants (Fig. 3a, black bars). The deleterious effects are not due to improper folding or impaired GTP binding of the mutant proteins, as the basal GTPase activities of most (36 of 40) of the mutant FtsY proteins are not significantly decreased (less than twofold) compared with wild-type FtsY (see Supplementary Table S1). The remaining four mutations decrease the basal GTPase activity to a greater, albeit still modest degree (3–8-fold; Supplementary Table S1). Nucleotide binding was not significantly affected in any of the mutants (data not shown).

When mapped onto the homologous residues in the structure of *T. aquaticus* FtsY in complex with Ffh (Fig. 3b), all of the mutants that have deleterious effects (red), with the exception of FtsY(K399(204)A) (where the number in parentheses relates to the homologous *T. aquaticus* sequence), lie within the FtsY–Ffh interface. This includes residues within conserved motifs in the GTPase site, the 'closing loop' that packs against the guanine base, and the N–G domain interface. All of the neutral mutants (Fig. 3b, yellow) lie on the opposite side, pointing into solvent and away from the interface. Thus, the extensive interaction surface seen in the structure is functionally important for the stability and/or activity of the complex.

### Conformational change that activates both GTPases

Superposition of the structures of FtsY·GMPPNP and Ffh·NG·GMPPNP on the heterodimeric complex shows that, on complex formation, the highly conserved motifs II (133–145; IBD loop) and III (187–192) in each G domain undergo major conformational rearrangements as they seal the upper part and lateral entrance of the catalytic sites from solvent water (Fig. 4a, b). As a consequence, the two IBD loops each bring three key side chains into the active

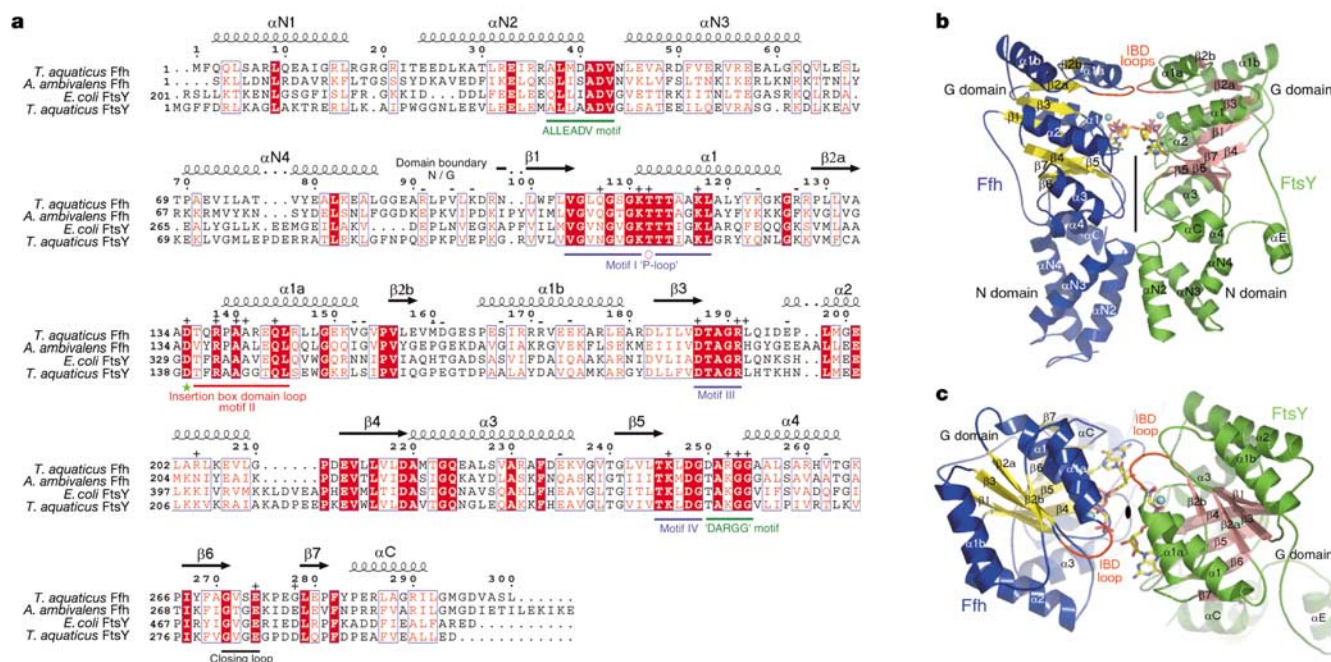


**Figure 1** Sequence alignment of SRP GTPases of known structure, and structure of the FtsY–Ffh heterodimer. **a**, Sequences of Ffh (*T. aquaticus* and *Acidianus ambivalens*) and FtsY (*E. coli* and *T. aquaticus*). Conserved regions (red) include motifs I (P-loop), II, III and IV, the closing loop, the ALLEADV and DARGG motifs, T112 (red circle) and D135 (asterisk). Residues of similar chemical nature (boxed in blue) and secondary structure elements are indicated. Mutations (see Fig. 3a) affecting GTPase activity (+) and neutral mutations (–) are also indicated. Numbering in the text is the residue and number within its own sequence, followed in brackets by the residue if different and the number of the

homologous residue in *T. aquaticus* Ffh, which we use as a reference for all SRP GTPases. *E. coli* FtsY contains an additional N-terminal domain, of unknown function, that is absent in *T. aquaticus* FtsY. **b**, **c**, The heterodimer shown in two orientations. Blue and yellow colouring of Ffh indicate α-helices and β-strands; the corresponding structures in FtsY are shown in green and pink. The quasi-two-fold axis is indicated in black. The two bound GMPPCP molecules (yellow sticks) coordinated to two Mg<sup>2+</sup> ions (cyan spheres), and the IBD loops (red), are shown. See Supplementary Information for a movie of the structure.

site of their respective protein (see below) and also contribute to the heterodimerization interface.

A highly conserved interface consisting of the ALLEADV motif within the N domain and the 'DARGG' motif within the G domain acts as a fulcrum that allows readjustment of the relative position of the N and G domains. Both N domains also change conformation on complex formation, bending towards the quasi-two-fold axis and approaching closest contact at the level of the N–G domain interface (Fig. 2b, grey arrows). These changes are coupled to the G domains through extensive interactions across the N–G interface by means of the DARGG motifs. As a consequence, conserved motif IV is brought into closer contact with the guanine base. In particular the specificity determinant D258(248) in FtsY optimizes hydrogen bonding with the N2 and N3 amino groups (the average hydrogen bond distance is 2.7 versus 3.4 Å in the complex of FtsY–Ffh versus free FtsY). This rearrangement explains the observation that FtsY acquires substantial nucleotide specificity only on its association with Ffh<sup>23</sup>.

## Substrate twinning at a composite active site

### Trans-substrate interactions

The two GTPase sites are paired to form a composite active site at the interface between FtsY and Ffh. The extended analogues lie

approximately perpendicular to the quasi-two-fold axis. Thus, the two GMPPCPs are twinned to face each other in a head-to-tail manner (Figs 1b, c and 2b, red arrows). To our knowledge, such a direct nucleotide–nucleotide association is unprecedented. The two nucleotides are sequestered from bulk solvent and bound such that the  $\gamma$ -phosphate of each GMPPCP accepts a 2.6 Å hydrogen bond from the 3'OH of the ribose ring of the other GMPPCP (Fig. 5). The ribose sugar pucker is C3'-endo in both cases, providing ideal geometry of the OH donor, and makes the active site reciprocal in atomic detail. This is the primary contact between active sites across the heterodimer interface.

To test the role of the *trans*-substrate interactions between the ribose 3'OH groups and the  $\gamma$ -phosphate oxygens, we determined the effect of removing the hydrogen bond donor by replacing the 3'OH of each GTP with 3'H. This was facilitated by the use of *E. coli* mutant Ffh and FtsY, which have altered nucleotide specificity for XTP (xanthosine 5'-triphosphate) instead of GTP (Ffh(D251(248)N) and FtsY(D449(248)N))<sup>14,23</sup>. Use of the mutants allows selective occupation of one of the GTPase sites with GTP or GTP analogues, and permits comparisons of their ability to stimulate the rate of XTP hydrolysis on the partner.

Figure 3c shows the stimulation of XTP hydrolysis on mutant FtsY(D449(248)N) by Ffh molecules bound with GTP analogues.

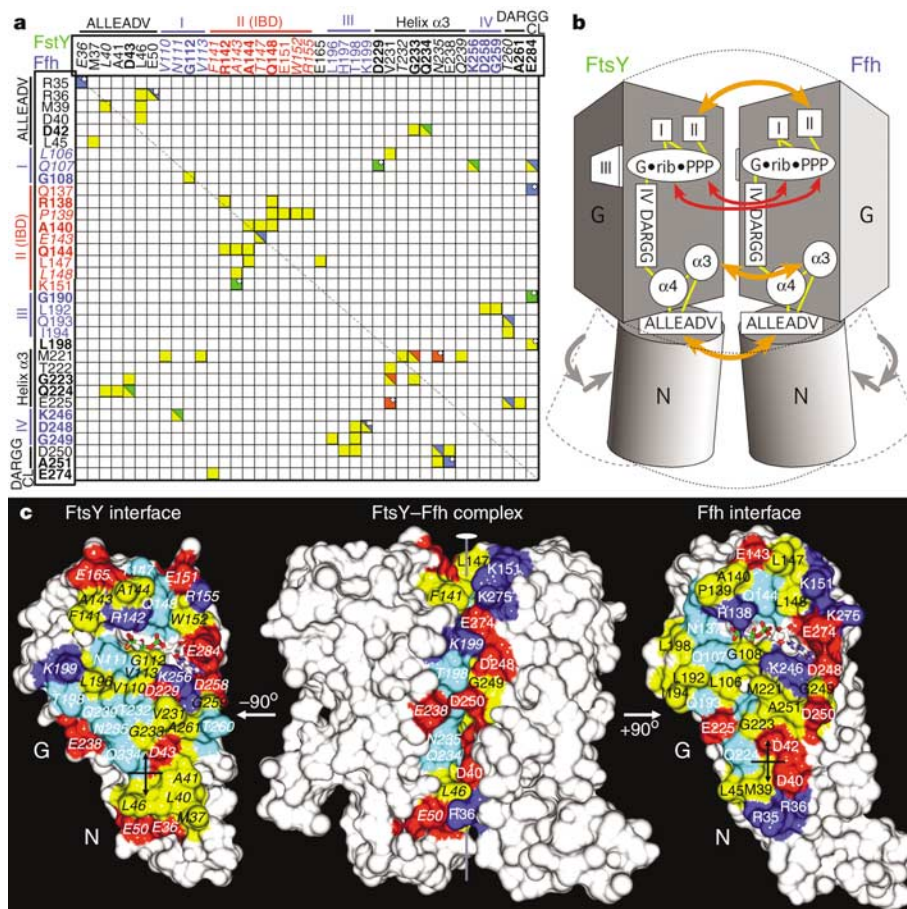


**Figure 2** The heterodimerization interface. **a**, Inter-residue contacts represented in a matrix. Van der Waals contacts (yellow) and hydrogen bonds (blue for side chain to side chain, green for side chain to backbone, and red for backbone to backbone) are shown. Water-mediated hydrogen bonds or ionic interactions are represented as white dots and white squares, respectively. Residue numbers and the conserved motifs are indicated. Residues indicated in bold are strictly conserved in both proteins. Symmetry across the diagonal emphasizes the quasi-two-fold symmetry. **b**, Interactions in the interface (orange

arrows), nucleotide twinning (red arrows) and rearrangements (grey arrows). Motifs I, II, III and IV are involved in nucleotide-binding and/or catalysis. The helices  $\alpha$ 4 act as adaptors between the N and G domains. **c**, Surface complementarity. The complex (middle) is opened  $-90^\circ$  (FtsY, left) and  $+90^\circ$  (Ffh, right). GMPPCP (in sticks) and side chains (positive, blue; negative, red; hydrophobic, yellow; hydrophilic, cyan) are mapped. The cross shows a point of contact on the quasi-two-fold axis (vertical). FtsY residues are italicized whereas Ffh residues are not.



We followed the reaction  $\text{XTP} + \text{FtsY(D449(248)N)} + \text{Ffh} \cdot \text{NTP} \rightarrow \text{XDP} + \text{P}_i$  (where NTP denotes GTP or GTP analogues and  $\text{P}_i$  denotes the phosphate anion), which includes effects on both Ffh–FtsY complex formation and activation of XTP hydrolysis. When Ffh is bound with 3'dGTP (Fig. 3c, filled circles) rather than GTP (triangles), the rate constant of this reaction is reduced 420-fold. In contrast, replacing the 2'OH of GTP with 2'H has only a twofold effect (Fig. 3c, open circles).

The same result holds for the reciprocal reaction; that is, the stimulation of XTP hydrolysis on mutant Ffh(D251(248)N) by FtsY molecules bound with GTP analogues ( $\text{XTP} \cdot \text{Ffh(D251(248)N)} + \text{FtsY} \cdot \text{NTP} \rightarrow \text{XDP} + \text{P}_i$ ) (Fig. 3d). Replacing the 3'OH of GTP by 3'H reduced the rate of the reaction by 140-fold (Fig. 3d, closed circles versus triangles), whereas replacement of the 2'OH by 2'H had less than a twofold effect (open circles). Thus the 3'OH of the GTP bound in each active site has a crucial role, contributing between 3.0 and 3.7 kcal mol<sup>-1</sup> to binding and reciprocal GTPase activation.

A water molecule between the  $\gamma$ -phosphate of GMPPCP in FtsY and the  $\alpha$ -phosphate of GMPPCP in Ffh also contributes to the interaction between nucleotides. The two CH<sub>2</sub> groups (7.1 Å between carbon atoms) and the two hydrophobic exo-faces of the ribose rings form a hydrophobic cavity with no electron density in

it. If GTP were bound, a water molecule(s), an ion, or a charged or polar side chain could fill the cavity, bridging oxygens of the  $\beta$ - and  $\gamma$ -phosphates. This additional interaction might contribute further to catalysis.

### Interactions between active site and substrate

Each active site provides catalytic groups for the bound nucleotide *in cis*. In each GMPPCP one oxygen of the  $\beta$ -phosphate and one oxygen of the  $\gamma$ -phosphate is coordinated by a single Mg<sup>2+</sup> ion in octahedral coordination with three water molecules and the OH group of a strictly conserved threonine residue from motif I (the 'P'-loop; T112 in Ffh and T116(112) in FtsY) (Fig. 5b). One water molecule in each GTPase lines up opposite the respective  $\beta$ – $\gamma$ -phosphate bonds in ideal attacking position for hydrolysis (Fig. 5a). These were not present in the separate FtsY·GMPPNP or Ffh·GMPPNP structures<sup>24</sup>. Each donates a hydrogen bond (2.6 Å) to a strictly conserved aspartate (D135 in Ffh and D139(135) in FtsY) from motif II (IBD loop; Fig. 5). These two aspartate residues also accept a hydrogen bond from one water molecule that coordinates the Mg<sup>2+</sup>. These aspartates are specific to the SRP family of GTPases and are the key, previously unrecognized catalytic groups that are only brought into correct orientation in the complex.

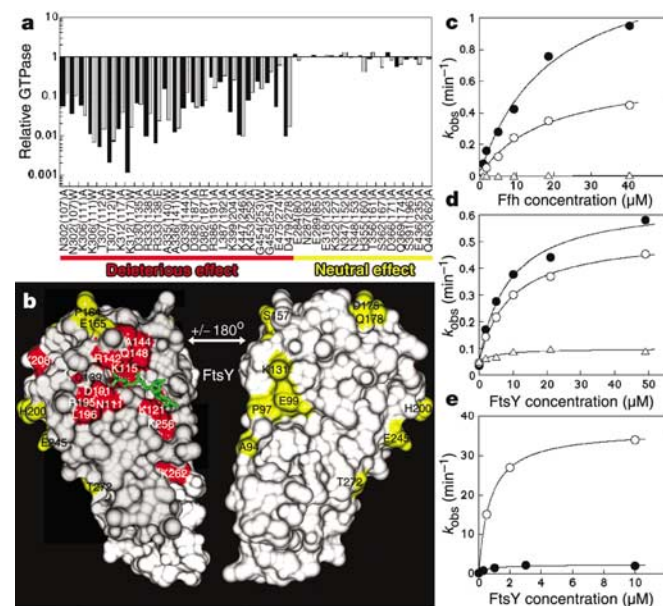


**Figure 3** Functional analysis of conserved residues and the 3'OH of GTP. **a**, The effect of FtsY mutations on the stimulated GTPase reaction. The dark and grey bars are the  $k_{\text{tot}}$  and  $k_{\text{cat}}$  values, respectively, for the mutant relative to wild-type FtsY. Red denotes mutants with deleterious effects whereas yellow denotes neutral mutants. **b**, Mutants in *E. coli* FtsY (coloured as in **a**) mapped onto the corresponding surface of complexed *T. aquaticus* FtsY. The interface (grey, left) with the bound nucleotide (green sticks) and the solvent-accessible side (white, right) are shown. **c, d**, Replacing the 3'OH of each GTP with 3'H compromises Ffh–FtsY association and reciprocal stimulation. XTP hydrolysis from XTP-specific mutants FtsY(D449(248)N) (**c**) or Ffh(D251(248)N) (**d**) were determined with the other GTPase active site bound by GTP (filled circles), 2'dGTP (open circles) or 3'dGTP (triangles). First-order fits to the linear portion of the concentration dependences gave apparent second-order rate constants ( $k_{\text{tot}}$ ) for XTP hydrolysis from FtsY(D449(248)N) (**c**) of  $6.0 \times 10^4$ ,  $2.6 \times 10^4$  and  $1.4 \times 10^2 \text{ M}^{-1} \text{ min}^{-1}$  with Ffh bound by GTP, 2'dGTP and 3'dGTP, respectively, and second-order rate constants for XTP hydrolysis from Ffh(D251(248)N) (**d**) of  $7.2 \times 10^4$ ,  $5.4 \times 10^4$  and  $5.3 \times 10^2 \text{ M}^{-1} \text{ min}^{-1}$  with FtsY bound by GTP, 2'dGTP and 3'dGTP, respectively. **e**, The stimulated GTPase reaction of mutant FtsY(D330(135)A) (filled circle) compared with the reaction of wild-type FtsY (open circle).

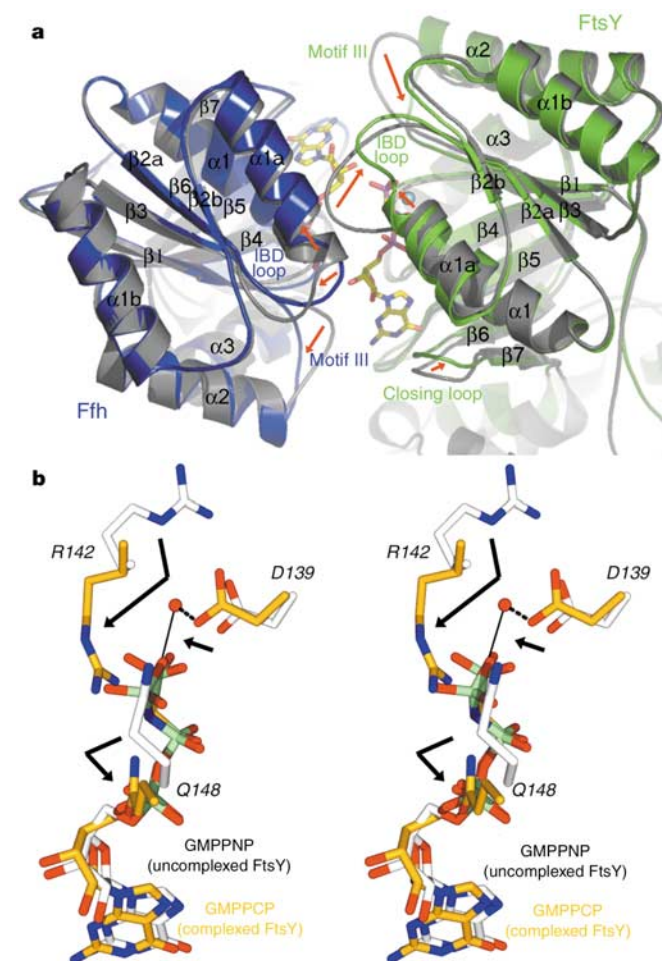


**Figure 4** Conformational rearrangements on formation of the FtsY–Ffh complex. **a**, Changes in the IBD and motif III regions. The structure of the GMPPCP-bound FtsY–Ffh complex (FtsY, green; Ffh, blue) is superposed on the GMPPNP-bound structures of FtsY and Ffh (grey). Red arrows highlight the rearrangements in particular in the helices  $\alpha 1a$  from the IBs. **b**, Structures of FtsY·GMPPCP from the FtsY–Ffh complex (orange) and free FtsY·GMPPNP (white) are superposed and show the changes (arrows) in the relative positions of the conserved residues D139(135), R142(138) and Q148(144).

Complex formation also brings R138 and Q144 of the Ffh IBD loop, and its conjugate pair of R142(138) and Q148(144) of the FtsY IBD loop, from far away into catalytic position in close contact with the  $\alpha$ -,  $\beta$ - and  $\gamma$ -phosphates of the GMPPCPs (Fig. 5b). These residues act to position the nucleotide for hydrolysis, and contribute to the electrostatic balance within the catalytic site where the negatively charged phosphate groups of the twinned GMPPCPs converge. Upon hydrolysis an extra negative charge is developed in each site, compromising this balance and destabilizing the complex. This notion is supported by the mechanism proposed for ABC transporters<sup>25</sup>, in which cooperative hydrolysis of two ATPs in a symmetrical homodimer drives domain dissociation, which in turn drives transport. However, in these structures the ATP substrates are far from each other and the mechanisms of coupling hydrolyses are different.

Additional symmetrical interactions involve close van der Waals contacts of side chains of R138 of Ffh with R142(138) and Q148(144) of FtsY and, reciprocally, of R142(138) of FtsY with R138 and Q144 of Ffh (Fig. 5b). In contrast, other conserved residues interact in ways that are not quite symmetrical. A hydrogen bond forms between the side chain of N111(Q107) of FtsY and the ribose 3' O of the GMPPCP bound to Ffh. This is matched—but not mirrored—by a van der Waals contact between Q107 of Ffh and the ribose ring of the GMPPCP bound to FtsY. Asparagine is strictly conserved in this position in all FtsY sequences and their eukaryotic orthologues; correspondingly, glutamine is conserved in all Ffh sequences and their eukaryotic orthologues. These two side chains are the only ones that interact with the opposing substrate. By breaking symmetry, they may be important in specifying the order of the two hydrolysis reactions in the SRP–SR heterodimer.

Consistent with the crucial role of the motif II loop in activation of the GTPases, mutations of residues in motif II (D135, R138, A140, A141 and Q144) all have deleterious effects (Fig. 3a). Figure 3e shows the effect of the D330(135)A mutation in *E. coli* FtsY. The first-order rate constant for the reaction  $\text{GTP} \cdot \text{FtsY} \cdot \text{Ffh} \cdot \text{GTP} \rightarrow \text{products}$  ( $k_{\text{cat}}$ ; Fig. 3a, grey bars), which measures the activation of GTP hydrolysis reaction after the complex is formed, is reduced 18-fold for FtsY(D330(145)A) compared with wild-type FtsY (Fig. 3e, compare filled with open circles). As the two active sites hydrolyse bound GTPs with the same rate constant in the complex<sup>14</sup>,

inactivation of only one of the GTPases would reduce the observed rate constant by only twofold. Thus, the large effect of the D330(135)A and other mutations (Fig. 3a, red) indicates that the activation of both GTPase sites is compromised, even when mutations are confined to one of the two GTPases. The proper assembly of the composite active site is therefore highly cooperative *in trans* between the two proteins.

## Discussion

The structure of the catalytic core of the SRP and SR complex suggests a unique mechanism by which nucleotide binding and hydrolysis drive complex formation and disassembly. The two proteins associate by means of an extensive interaction surface, which spans both the N and G domains, and undergo major conformational changes relative to the free proteins. Of the 40 mutations of surface residues that we made, 25 map to the interface and each shows a pronounced deleterious effect on complex formation. This indicates that the conformation of the protein in the complex is stable only when all required interactions are made. Thus, complex formation involves a highly cooperative and extensive network of interactions.

The closest related structures to the SRP GTPases include the homodimeric ATPase nitrogenase<sup>26</sup>. However, a model of the FtsY–Ffh complex<sup>20</sup> based on this failed to predict the N domain or mechanistic interactions. In contrast to most other GTPases, major rearrangements occur in Ffh and FtsY only as they associate in their GTP-bound forms. As free proteins, there are only subtle differences between the GTP- and GDP-bound states<sup>24</sup>. By contrast, other GTPases undergo marked rearrangements in response to GDP and GTP binding (for example, movements of 'switch regions' in motif II and motif III of Ras) and little further rearrangement takes place on binding their associated GTPase-activator proteins (GAPs).

The FtsY–Ffh complex forms a composite active site at the interface. In this site, many catalytic residues interact both with the substrate *in cis* and with residues across the interface *in trans*. As a result, complex formation and GTPase activation are highly coupled. Consistently, mutation of catalytic residues also impairs complex formation. Because of the composite nature of the active site, activation of each GTPase site is also highly coupled to

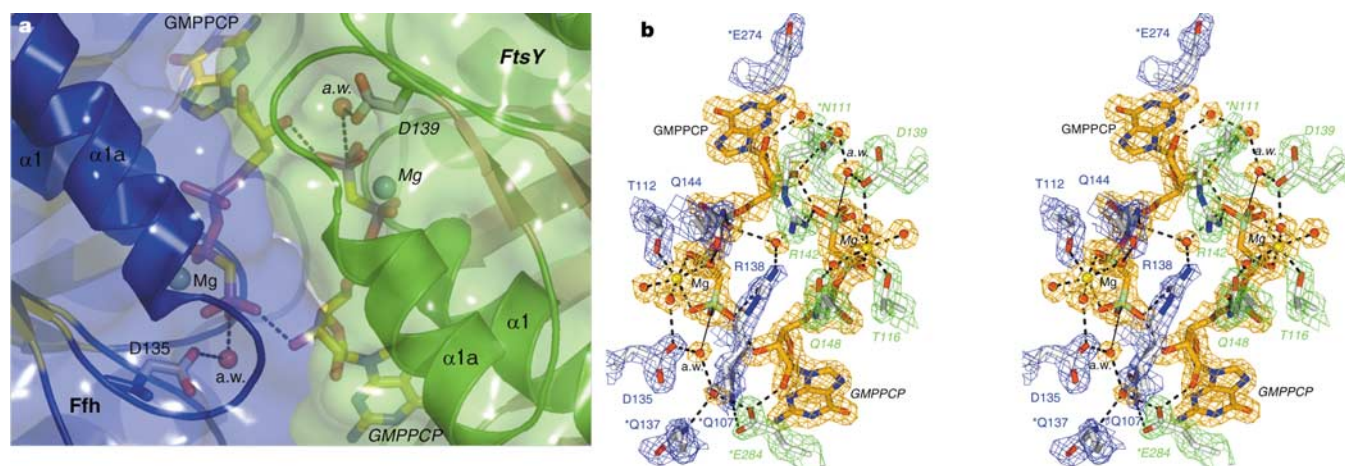


**Figure 5** The composite catalytic site with the twinned substrates and essential residues. **a**, The twinned substrates showing symmetrical hydrogen bonds between the 3' OH ribose of one GMPPCP and the  $\gamma$ -phosphate of the other GMPPCP. The two attacking waters (a.w.) are aligned for nucleophilic attack. Protein surfaces are blue (Ffh) or green (FtsY) transparent envelopes. **b**, Stereo view of the twinned catalytic site. The  $2F_o - F_c$  electron density map ( $2.1\sigma$ ) corresponding to Ffh (blue), FtsY (green) and ligands

(orange). Residues in Ffh (blue characters) and FtsY (green italic characters) are shown; asterisks indicate residues breaking the pseudo-symmetry. Black dashed lines indicate hydrogen bonds. Orientations in **a** and **b** are identical. See Supplementary Information for a movie showing the catalytic residues, the attacking waters and the twinned nucleotides.

activation of the other, as revealed by single mutations in the active site of one GTPase that inactivate both GTPases.

The structure suggests a unique activation mechanism for the SRP family of GTPases. Conformational rearrangements on complex formation bring catalytic residues in the IBD loop into the active site and align them with respect to the bound substrate. In particular D135 activates the attacking nucleophilic water molecule, and R138 and Q144 interact with the  $\beta$ - and  $\gamma$ -phosphate groups, and thus may contribute to stabilization of the transition state. The only catalytically important interactions between the GTPases are formed by the twinned substrates themselves, which further stabilizes the negative charge on the  $\gamma$ -phosphate groups. In contrast, the active sites of most GTPases become complemented on interaction with their respective GAPs through insertion of a missing catalytic residue, such as the 'arginine finger'. The only other known exceptions are the Ran<sup>27</sup> and G $\alpha$  GTPases<sup>28–30</sup>, which on activation align key catalytic residues *in cis*.

The extensive interactions with the  $\gamma$ -phosphate group, both from active-site residues *in cis* and from the twinned substrate *in trans*, explain why complex formation is GTP-dependent and why GTP hydrolysis leads to complex dissociation. Hydrolysis of GTP releases the  $\gamma$ -phosphate, and therefore severs the connections with both the substrate and active-site residues. Electrostatic repulsion between the released phosphate and GDP might assist further in dissociating the partners. The most basic requirement for SRP-dependent unidirectional targeting, namely the obligatory coupling of the formation of a tight SRP–SR complex with its subsequent disassembly, is therefore elegantly explained by these structural and functional analyses.

**Note added in proof:** A structure of the complex reported here in a different crystal form has been determined independently<sup>31</sup>. No information was shared prior to publication. □

## Methods

### Protein preparation

Full-length FtsY (residues Met 1 to Asp 304) and the N and G domains of Ffh (residues Met 1 to Leu 300) from *T. aquaticus* were expressed in BL21(DE3)–Rosetta *E. coli* cells, and subcloned in the pET28b vector as N-terminal hexa-histidine fusions. Proteins were expressed at 37 °C in LB medium. Soluble cellular extracts were heated at 70 °C for 30 min and clarified by centrifugation. FtsY and Ffh-NG were purified by metal affinity chromatography followed by gel filtration. The thrombin-cleavable histidine tags were removed. The FtsY–Ffh-NG binary complex was formed by incubation of stoichiometric amounts of FtsY and Ffh-NG in the presence of a twofold excess of the non-hydrolysable GTP analogue GMPPCP. The complex was purified by gel filtration and concentrated for crystallization. Expression plasmids for mutant FtsYs were constructed from wild-type *E. coli* FtsY(47–497). Truncation of the first 46 amino acids improves expression and has no discernible effect on the interaction with Ffh or on the GTPase activity of FtsY alone or complexed to Ffh. Mutant FtsYs were expressed and purified as for wild type<sup>22</sup>.

### Crystallization and structure determination

The complex was crystallized by vapour diffusion at 4 °C using the Nextal crystallization pre-filled screening suites and tools (Nextal Biotechnologies). Crystals grew in 10% PEG 8,000 and 100 mM HEPES, pH 7.5, or 10% PEG 20,000 and 100 mM MES, pH 6.5, and were optimized at 4 °C and at 20 °C combining seeding and additive screening. Crystals were flash-frozen using mother liquor supplemented with 25% glycerol. Diffraction data collected at beamline 8.3.1 at the Advanced Light Source (ALS) at LBNL were integrated and scaled with DENZO and SCALEPACK<sup>32</sup>. The space group is  $P2_12_1$  with unit cell dimensions  $a = 75.0$  Å,  $b = 83.7$  Å,  $c = 94.0$  Å with one heterodimer per asymmetrical unit. The structure was solved by molecular replacement using the crystal structures of Ffh-NG and FtsY bound to GMPPNP as search models in AmoRe<sup>33</sup>. Refinement in CNS<sup>34</sup> and model building in Moloc<sup>35</sup> yielded the structure consisting of FtsY (residues Asn 27 to Glu 303), Ffh (residues Gly 19 to Gly 295), two GMPPCP molecules and 387 water molecules. All residues are in the most allowed regions of the Ramachandran diagram. On complex formation only, there is enhanced hydrolysis of the first 25 residues of FtsY as previously noted<sup>36</sup> and as also seen here by mass spectrometry. These residues are removed perhaps by self-cleavage within the sequence G24–G25–N26. Before complex formation this variable region of the N domain of FtsY–GMPPNP is relatively unstructured. Whether this is important functionally is not yet known. The first 18 residues of the NG domain of Ffh are present but poorly ordered in the structure. Figures were prepared with PyMol<sup>37</sup> and DINO<sup>38</sup>.

### Kinetic analysis of the Ffh–FtsY interaction

Stimulated GTP hydrolyses by *E. coli* Ffh and FtsY were followed by monitoring

radioactive  $P_i$  release<sup>23</sup>. An approximately twofold excess of 4.5S RNA over Ffh was present to facilitate the Ffh–FtsY complex formation. The reciprocally stimulated GTPase reactions were determined in multiple turnover experiments ( $[GTP] > [Ffh + FtsY]$ ). Varying amounts of wild-type or mutant FtsY were added to a small, fixed amount of Ffh (0.05–0.1  $\mu$ M) in the presence of a saturating amount of GTP (100  $\mu$ M) to occupy both GTPase active sites ( $K_d^{GTP} = 0.39$  for Ffh;  $K_d^{GTP} = 14$   $\mu$ M for FtsY). Nucleotide affinity of FtsY was not significantly affected by any of the mutations reported here. The concentration-dependence of FtsY was analysed<sup>22</sup> to obtain rate constants  $k_{tot}$  and  $k_{cat}$  for the summed GTP hydrolyses.  $k_{tot}$  is identical to the operationally defined second-order rate constant referred to as  $k_{cat}/K_m$  in previous work<sup>22</sup>.

XTP hydrolysis from mutant FtsY(D449(248)N) was determined in single-turnover reactions ( $[XTP] < [E]$ ) with a fixed, subsaturating amount of FtsY(D449(248)N) (0.2  $\mu$ M) with respect to XTP ( $K_d^{XTP} = 260$   $\mu$ M)<sup>24</sup>, and varying amounts of Ffh. A 50  $\mu$ M concentration of GTP or GTP analogues was present to selectively saturate the GTPase site in Ffh ( $K_d^{GTP} = 0.39$   $\mu$ M;  $K_d^{3'dGTP} = 0.63$   $\mu$ M;  $K_d^{2'dGTP} = 0.86$   $\mu$ M). The reaction  $XTP + FtsY(D449(248)N) + Ffh-NTP \rightarrow XDP + P_i$  was followed by radioactive  $P_i$  release from XTP. The apparent second-order rate constant for the reaction ( $K_{tot}^{app}$ ) was obtained from the slope of the initial linear portion of the dependence on concentration of Ffh.

The reciprocal reaction, XTP hydrolysis from mutant Ffh(D251(248)N), was determined in single-turnover experiments with a fixed, saturating amount of Ffh(D251(248)N) (2  $\mu$ M) with respect to XTP ( $K_d^{XTP} = 0.31$   $\mu$ M; S.-o.S. and P.W., unpublished observations) and varying amounts of FtsY. A concentration of 200  $\mu$ M GTP or GTP analogues (NTPs) was present to selectively occupy the GTPase site in FtsY ( $K_d^{3'dGTP} = 52$   $\mu$ M;  $K_d^{2'dGTP} = 32$   $\mu$ M). Thus, the reaction  $XTP-Ffh(D251(248)N) + FtsY-NTP \rightarrow XDP + P_i$  was followed. The rate constant for this reaction,  $k_{tot}$ , was obtained from the slope of the initial linear portion of the dependence on the concentration of FtsY.

Received 25 August; accepted 25 November 2003; doi:10.1038/nature02250.

- Keenan, R. J., Freymann, D. M., Stroud, R. M. & Walter, P. The signal recognition particle. *Annu. Rev. Biochem.* **70**, 755–775 (2001).
- Stroud, R. M. & Walter, P. Signal sequence recognition and protein targeting. *Curr. Opin. Struct. Biol.* **9**, 754–759 (1999).
- Pool, M. R., Stumm, J., Fulga, T. A., Sinning, I. & Dobberstein, B. Distinct modes of signal recognition particle interaction with the ribosome. *Science* **297**, 1345–1348 (2002).
- Rinke-Appel, J. *et al.* Crosslinking of 4.5S RNA to the *Escherichia coli* ribosome in the presence or absence of the protein Ffh. *RNA* **8**, 612–625 (2002).
- Gilmore, R., Blobel, G. & Walter, P. Protein translocation across the endoplasmic reticulum. I. Detection in the microsomal membrane of a receptor for the signal recognition particle. *J. Cell Biol.* **95**, 463–469 (1982).
- Meyer, D. I., Krause, E. & Dobberstein, B. Secretory protein translocation across membranes—the role of the 'docking protein'. *Nature* **297**, 647–650 (1982).
- Walter, P. & Blobel, G. Purification of a membrane-associated protein complex required for protein translocation across the endoplasmic reticulum. *Proc. Natl Acad. Sci. USA* **77**, 7112–7116 (1980).
- Gilmore, R., Walter, P. & Blobel, G. Protein translocation across the endoplasmic reticulum. II. Isolation and characterization of the signal recognition particle receptor. *J. Cell Biol.* **95**, 470–477 (1982).
- Beckmann, R. *et al.* Alignment of conduits for the nascent polypeptide chain in the ribosome–SecE1 complex. *Science* **278**, 2123–2126 (1997).
- Menetret, J. F. *et al.* The structure of ribosome–channel complexes engaged in protein translocation. *Mol. Cell* **6**, 1219–1232 (2000).
- Beckmann, R. *et al.* Architecture of the protein-conducting channel associated with the translating 80S ribosome. *Cell* **107**, 361–372 (2001).
- Miller, J. D., Wilhelm, H., Gierach, L., Gilmore, R. & Walter, P. GTP binding and hydrolysis by the signal recognition particle during initiation of protein translocation. *Nature* **366**, 351–354 (1993).
- Miller, J. D., Bernstein, H. D. & Walter, P. Interaction of *E. coli* Ffh/4.5S ribonucleoprotein and FtsY mimics that of mammalian signal recognition particle and its receptor. *Nature* **367**, 657–659 (1994).
- Powers, T. & Walter, P. Reciprocal stimulation of GTP hydrolysis by two directly interacting GTPases. *Science* **269**, 1422–1424 (1995).
- Keenan, R. J., Freymann, D. M., Walter, P. & Stroud, R. M. Crystal structure of the signal sequence binding subunit of the signal recognition particle. *Cell* **94**, 181–191 (1998).
- Montoya, G., Svensson, C., Lührink, J. & Sinning, I. Crystal structure of the NG domain from the signal-recognition particle receptor FtsY. *Nature* **385**, 365–368 (1997).
- Freymann, D. M., Keenan, R. J., Stroud, R. M. & Walter, P. Structure of the conserved GTPase domain of the signal recognition particle. *Nature* **385**, 361–364 (1997).
- Ramirez, U. D. *et al.* Structural basis for mobility in the 1.1 Å crystal structure of the NG domain of *Thermus aquaticus* Ffh. *J. Mol. Biol.* **320**, 783–799 (2002).
- Vetter, I. R. & Wittinghofer, A. The guanine nucleotide-binding switch in three dimensions. *Science* **294**, 1299–1304 (2001).
- Montoya, G., Kaat, K., Moll, R., Schafer, G. & Sinning, I. The crystal structure of the conserved GTPase of SRP54 from the archaeon *Acidianus ambivalens* and its comparison with related structures suggests a model for the SRP–SRP receptor complex. *Struct. Fold. Des.* **8**, 515–525 (2000).
- Rapiejko, P. J. & Gilmore, R. Empty site forms of the SRP54 and SR  $\alpha$  GTPases mediate targeting of ribosome–nascent chain complexes to the endoplasmic reticulum. *Cell* **89**, 703–713 (1997).
- Peluso, P., Shan, S. O., Nock, S., Herschlag, D. & Walter, P. Role of SRP RNA in the GTPase cycles of Ffh and FtsY. *Biochemistry* **40**, 15224–15233 (2001).
- Shan, S. & Walter, P. Induced nucleotide specificity in a GTPase. *Proc. Natl Acad. Sci. USA* **100**, 4480–4485 (2003).
- Padmanabhan, S. & Freymann, D. M. The conformation of bound GMPPNP suggests a mechanism for gating the active site of the SRP GTPase. *Structure* **9**, 859–867 (2001).

25. Smith, P. C. *et al.* ATP binding to the motor domain from an ABC transporter drives formation of a nucleotide sandwich dimer. *Mol. Cell* **10**, 139–149 (2002).
26. Schindelin, H., Kisker, C., Schlessman, J. L., Howard, J. B. & Rees, D. C. Structure of ADP × AIF4(–)-stabilized nitrogenase complex and its implications for signal transduction. *Nature* **387**, 370–376 (1997).
27. Seewald, M. J., Korner, C., Wittinghofer, A. & Vetter, I. R. RanGAP mediates GTP hydrolysis without an arginine finger. *Nature* **415**, 662–666 (2002).
28. Tesmer, J. J., Berman, D. M., Gilman, A. G. & Sprang, S. R. Structure of RGS4 bound to AIF4-activated Gi α1: Stabilization of the transition state for GTP hydrolysis. *Cell* **89**, 251–261 (1997).
29. Srinivasa, S. P., Watson, N., Overton, M. C. & Blumer, K. J. Mechanism of RGS4, a GTPase-activating protein for G-protein α subunits. *J. Biol. Chem.* **273**, 1529–1533 (1998).
30. Slep, K. C. *et al.* Structural determinants for regulation of phosphodiesterase by a G protein at 2.0 Å. *Nature* **409**, 1071–1077 (2001).
31. Focia, P. J., Shepotinovskaya, I. V., Seidler, J. A. & Freymann, D. M. Heterodimeric GTPase core of the SRP targeting complex. *Science* (in the press).
32. Otwinowski, Z. & Minor, W. Processing X-ray data in oscillation mode. *Methods Enzymol.* **276**, 307–326 (1996).
33. Navaza, J. Implementation of molecular replacement in AMoRe. *Acta Crystallogr. D* **57**, 1367–1372 (2001).
34. Brunger, A. T. *et al.* Crystallography & NMR system: A new software suite for macromolecular structure determination. *Acta Crystallogr. D* **54**, 905–921 (1998).
35. Muller, K. *et al.* Moloc. *Bull. Soc. Chim. Belg.* **97**, 655–667 (1988).
36. Shepotinovskaya, I. V. & Freymann, D. M. Conformational change of the N-domain on formation of

the complex between the GTPase domains of *Thermus aquaticus* Ffh and FtsY. *Biochim. Biophys. Acta* **1597**, 107–114 (2002).

37. DeLano, W. L. *The PyMOL Molecular Graphics System* (<http://www.pymol.org/>) 2003).
38. Philippsen, A. DINO: *Visualizing Structural Biology* (<http://www.dino3d.org/>) (2002).

**Supplementary Information** accompanies the paper on [www.nature.com/nature](http://www.nature.com/nature).

**Acknowledgements** We thank C. Reyes for invaluable contributions to the initial FtsY mutant design and structure determination of *T. aquaticus* FtsY-GMPPNP, and R. Vale, H. Bourne and N. Bradshaw for comments on the manuscript. We acknowledge K. Slep and L. Rice for discussion and advice, and thank J. Holton and G. Meigg for support during data collection at the Advanced Light Source. D.F.S. was supported by a Burroughs-Wellcome Fund graduate fellowship. S.S. is supported by a Damon Runyan/Walter Winchell Cancer research fellowship. This work was supported by NIH grants to R.M.S. and P.W. P.W. is an Investigator of the Howard Hughes Medical Institute.

**Competing interests statement** The authors declare that they have no competing financial interests.

**Correspondence** and requests for materials should be addressed to R.M.S. (stroud@msg.ucsf.edu) or P.E.E. (pascal@msg.ucsf.edu). Coordinates for the FtsY–Ffh heterodimer complex bound to GMPPCP have been deposited in the Protein Data Bank under accession code 1R9J.